Wakepotentials of the CompactLight X-band and C-band LINAC

Evan Ericson

Supervisor: Xiaowei Wu

CERN Summer Student
June-August 2021

Abstract

In this report, the transverse wakepotential of the CompactLight X-band LINAC were computed after a mesh convergence study was performed. Simulations done here reproduced results found previously but used a coarser mesh and thus a smaller computational load. The transverse and longitudinal impedances of the X-band structure are reported. The longitudinal wakepotential of the CompactLight X-band LINAC were computed as well. Mesh convergence studies were performed on the CompactLight C-band structure to determine a suitable mesh. The transverse and longitudinal wakepotentials and impedances of the CompactLight C-band LINAC were computed. The transverse wakepotential of the C-band structure was reproduced by combining the wakes resulting from constant impedance structures.

Introduction

The CompactLight Project's goal is to utilize high gradient radio frequency (RF) linear accelerators (LINAC) to provide an X-ray free electron laser (XFEL) with a smaller footprint and electrical power requirement than current XFEL's resulting in lower overall cost. The design begins with a common a C-band photoinjector, C-band LINAC, bunch compressors and X-band LINAC before branching into 2 separate undulator lines (see Figure 1. The facility aims to have 2 modes of operation in order to provide hard and soft X-rays to users.

The X-band LINAC accelerates the electron beam from 300 MeV to 2 GeV. The main parameters are summarized in Table 1. Each LINAC consists of 4 RF accelerating structures. The focus of this report is to quantify the wakefields of the X-band and C-band structures comprising the CompactLight LINAC.

Parameter	Unit	Soft X-ray	Hard X-ray
Repetition rate [1]	Hz	1000	100
Avg. C-band gradient [2]	MV/m	15	
Avg. X-band gradient [3]	MV/m	30.4	65

Table 1: Operating parameters of CompactLight's LINACs

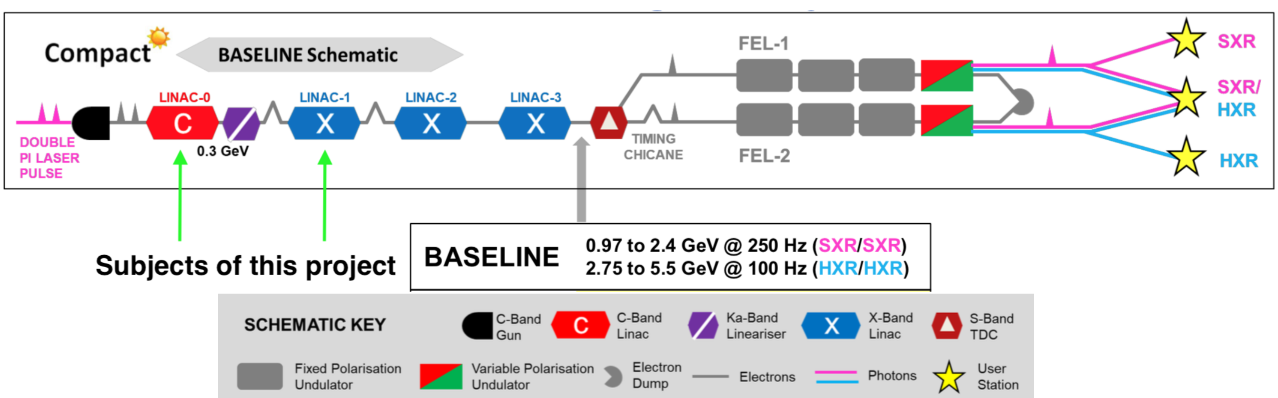

Figure 1: Overview of the CompactLight accelerator complex.

X-band structure

The transverse wakefields of the CompactLight X-band structures were previously determined [4]. The results, which agreed with theory, were used to minimize the wakefield effects at the position of a second bunch. A fine mesh of 0.02 mm and extra mesh planes were included to accurately model the structure with particular attention to accurately representing the structure's irises whose thicknesses varied along the

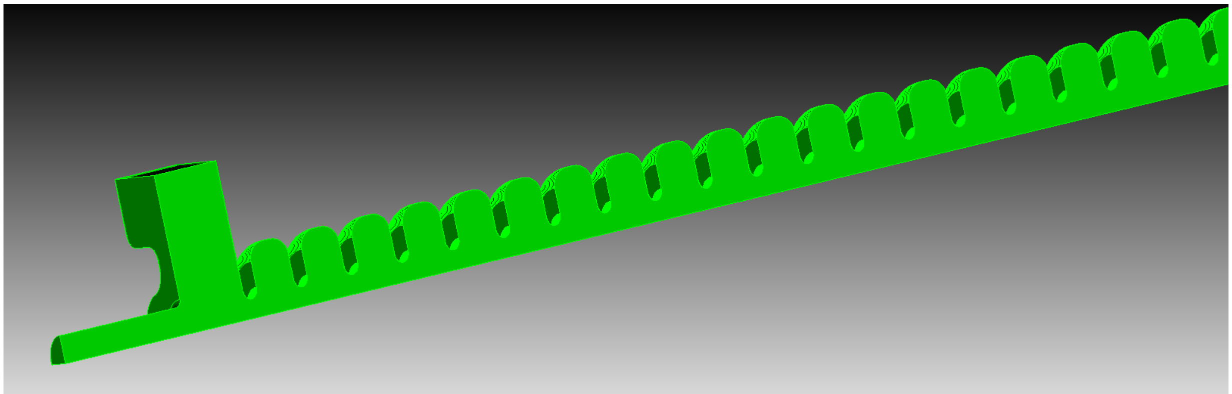

Figure 2: 3D model of the CompactLight X-band accelerating structure.

Parameter	Unit	Value
structure length	mm	970
cells per structure	-	109
cell length	mm	8.332
iris radius	mm	4.3-2.7
iris thickness	mm	2.00-2.24
outer cell rounding	mm	2.5

Table 2: CompactLight X-band structure geometry [2, 3]

length of the structure. Determining the minimum mesh requirements to reproduce the previous results will expedite future wakefield studies of similar structures. The geometry of the X-band structure is summarized by the by quantities in Table 2 and a model is shown in 2

Mesh convergence studies determine the largest mesh required for a simulation to provide accurate results. The mesh representing a geometry is progressively refined until refining the mesh no longer results in a change to the simulation output; at this point the mesh is said to have converged. Examples of the same geometry with two different mesh sizes are shown in Figure 3.

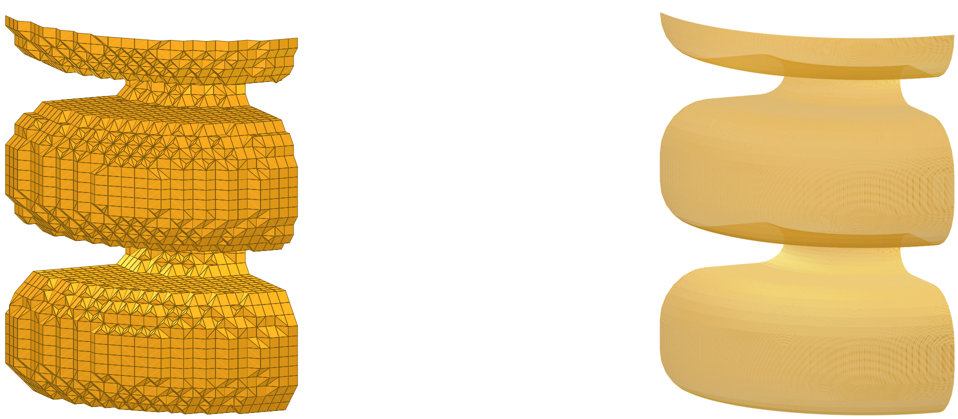

(a) (b)

Figure 3: Comparison of mesh coarseness on a portion of the X-band structure. The plots were produced in GdfidL. (a) Mesh of 0.50 mm. (b) Mesh of 0.02 mm.

Transverse Wakefields

Figure 4 compares the transverse wakepotentials of a portion of the X-band structure produced using two different mesh sizes. Despite relatively good agreement, the two wakepotentials differ noticeably near the 10th RF cycle at 0.83 ns, a potential time of the second bunch [4].

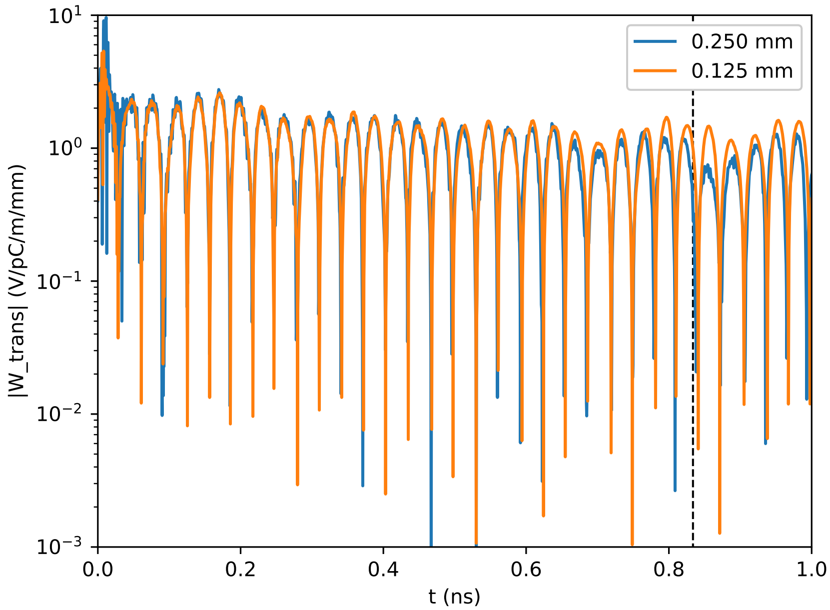

Figure 4: Transverse wakepotential of CompactLight X-band structure using 36 mm of the structure. The 10^{th} RF cycle, the position of a witness bunch, is represented by a vertical dashed line.

The results of simulations using finer mesh setting are shown in Figure 5. The transverse wakepotential of a simulation done with a mesh of 0.125 mm shows some disagreement with simulations done with finer mesh at very short time scales. A mesh of 0.0625 mm was chosen to provide an accurate transverse wakepotential for the CompactLight X-band accelerating structure.

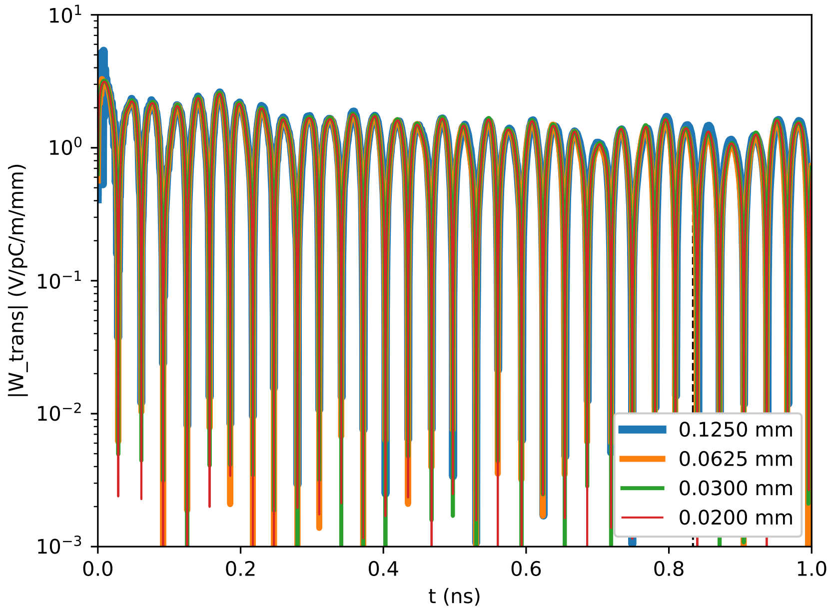

Figure 5: Mesh convergence of transverse wakepotential of CompactLight X-band structure using 36 mm of the structure.

Figure 6 shows the transverse wakepotential of a X-band structure produced by a bunch with $\sigma = 0.2$ mm. The wakepotential output from GdfidL had units of V/C. The wakepotential was scaled to V/pC/m/mm by diving the output by the length of the structure, the offset of the beam and a factor of 2. Since the excitation charge was on a magnetic plane, the simulation was done with half the charge specified in the input file and the resulting wakes needed to be divided by 2. One may look at Figure 6 and, for example, identify the valley near 0.2 ns as a wakepotential minimum and therefore a good time to inject a second bunch. However, any timing jitter will cause the witness bunch to see one of the wake's peaks adjacent to 0.2 ns. The wakepotential envelope follows the peaks of the wakepotential and is a conservative representation of the wakes and is plotted in Figure 6.

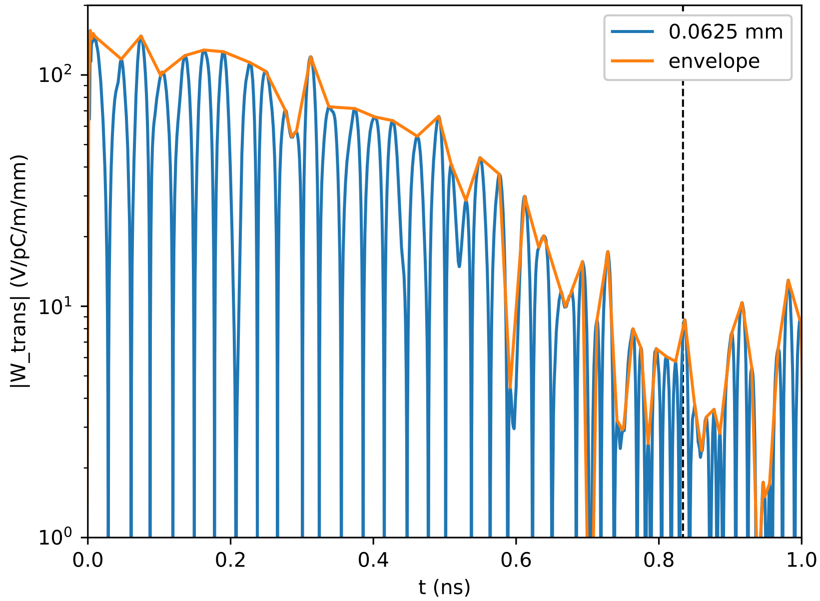

Figure 6: Transverse wakepotential of CompactLight X-band structure and a fit curve that removes oscillations.

The transverse impedance is shown in Figure 7 and agrees with the previously calculated impedance found using very fine mesh [4].

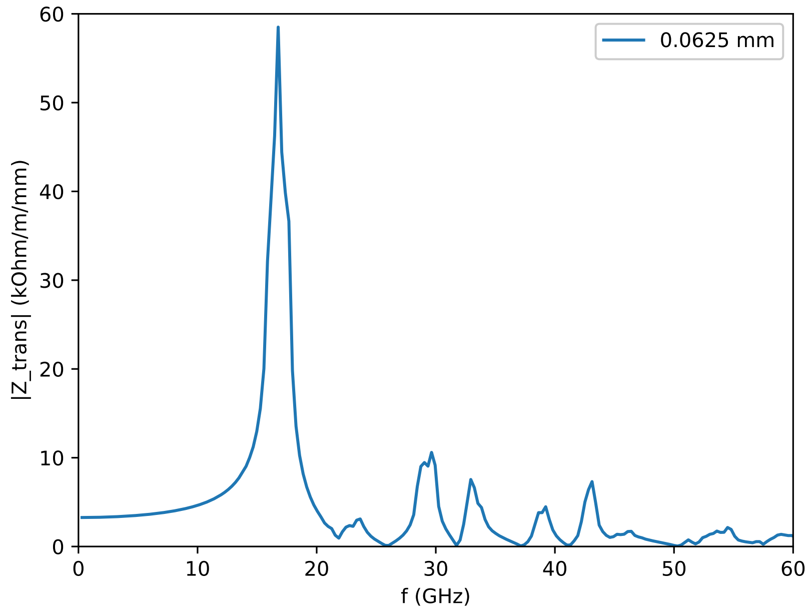

Figure 7: Transverse impedance of CompactLight X-band structure.

Longitudinal Wakefields

The results of mesh convergence study done on a portion of the accelerating structure shown in Figure 8 indicated a mesh of 0.0625 mm is sufficiently fine to provide an accurate longitudinal wakepotential for the CompactLight X-band accelerating structure.

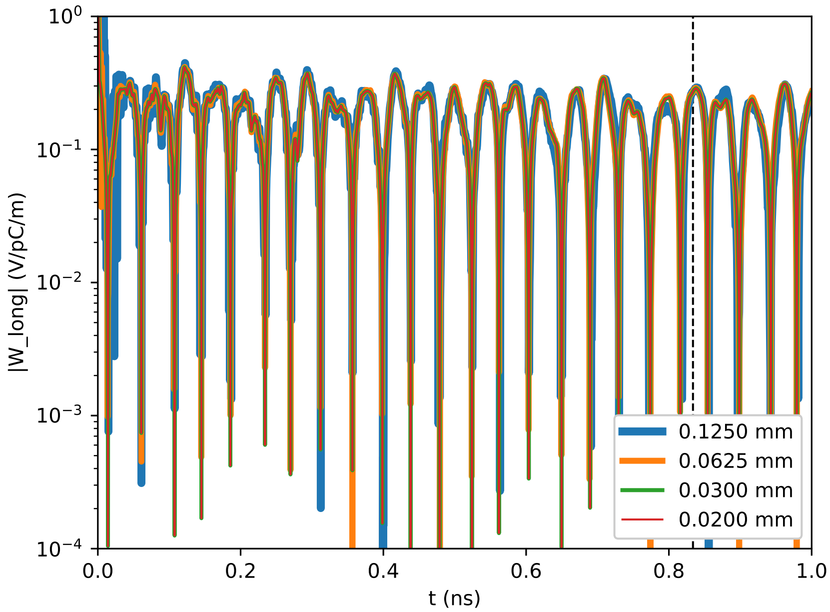

Figure 8: Mesh convergence of longitudinal wakepotential of CompactLight X-band structure using 36 mm of the structure.

Figure 9 shows the longitudinal wakepotential of a X-band structure produced by a bunch with $\sigma = 0.2$ mm and the wake envelope. The wakepotential output from GdfidL had units of V/C. The wakepotential was scaled to V/pC/m by diving the output by the length of the structure and a factor of 4. Since the excitation charge was on two magnetic planes, the simulation was done with a quarter the charge specified in the input file and the resulting wakes needed to be divided by 4.

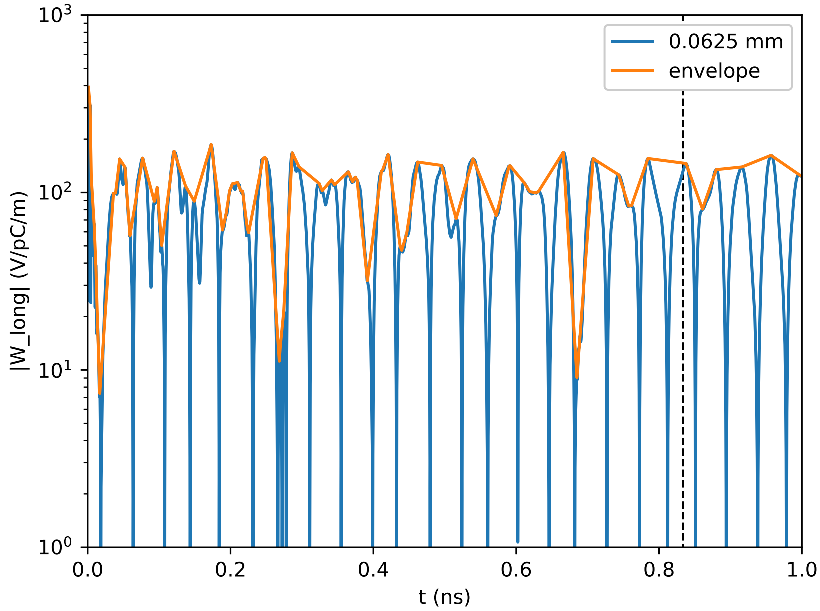

Figure 9: Longitudinal wakepotential of CompactLight X-band structure.

The longitudinal impedance is plotted in Figure 10.

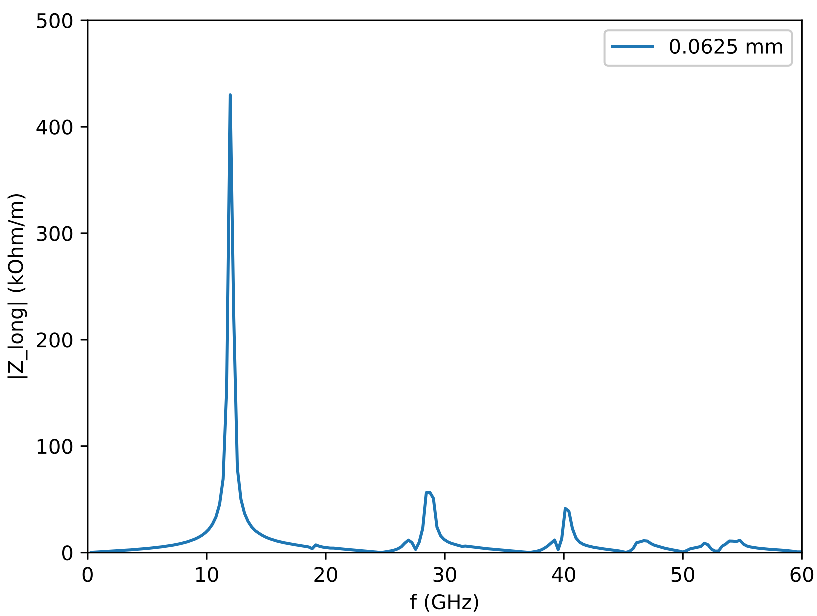

Figure 10: Longitudinal impedance of CompactLight X-band structure.

C-band structure

A model of a C-band accelerating structure needed to be made before simulations could be carried out. A model was constructed from a table of iris apertures a, and outer radii b the cell structure and a fixed iris thickness of $t = 4$ mm. Equations were fit to the table values to find a and b as functions of the cell number. The model built by implementing these equations into a script used by the modelling software Coreform Cubit is shown in Figure 11 while geometry parameters are summarized in Table 3.

Figure 11: CompactLight C-band structure model.

Parameter	Unit	Value
structure length	mm	2000
cells per structure	-	120
cell length	mm	16.67
iris radius	mm	6.94-6.26
iris thickness	mm	4
outer cell rounding	mm	5

Table 3: CompactLight C-band structure geometry [2]

Identical duplicates of the extreme upstream and downstream cells were added to the model to replicate matching cells. Mesh studies for the C-band structure began by doing wakefield simulations using a mesh of

$$\frac{0.0625\,\mathrm{mm}}{x} = \frac{5.996\,\mathrm{GHz}}{11.994\,\mathrm{GHz}} \tag{1}$$

$$x = 0.125020847\,\mathrm{mm} \simeq 0.125\,\mathrm{mm} \tag{2}$$

where 11.994 GHz is the operating frequency of the X-band structures and 5.996 GHz is the operating frequency of the C-band structures [2].

Transverse Wakefields

A comparison of the transverse wakes found using a mesh of 0.125 mm based on the estimate of Eq. (1) and a finer mesh is shown in Figure 12. The results agree relatively well. Because of the discrepancies between the wakes before 0.1 ns the finer mesh for simulating the transverse wakes of the entire structure was preferred.

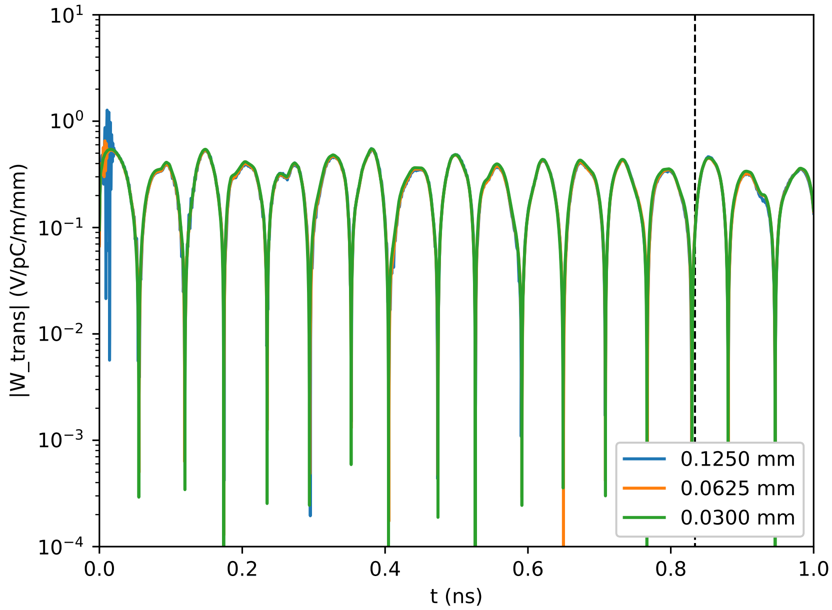

Figure 12: Transverse wakepotential of CompactLight C-band structure using 46 mm of the structure.

The results using finer mesh are shown in Figure 13. The difference between the wakes calculated using 0.0625 mm and 0.03 mm is negligible. A mesh of 0.0625 mm is sufficient to accurately calculate the transverse wakes of the C-band structure.

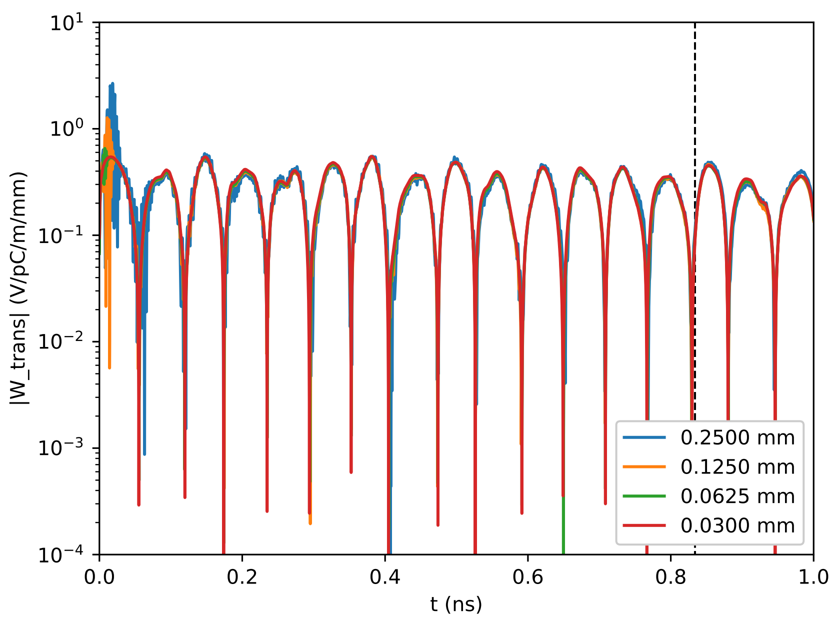

Figure 13: Transverse wakepotential of CompactLight C-band structure using 46 mm of the structure.

Figure 14 shows the transverse wakepotential of a C-band structure produced by a bunch with σ = 0.2 mm. The wakepotential output from GdfidL had units of V/C. The wakepotential was scaled to V/pC/m/mm by diving the output by the length of the structure, the offset of the beam and a factor of 2. Since the excitation charge was on a magnetic plane, the simulation was done with half the charge specified in the input file and the resulting wakes needed to be divided by 2. The transverse impedance of the C-band structure are shown in Figure 15.

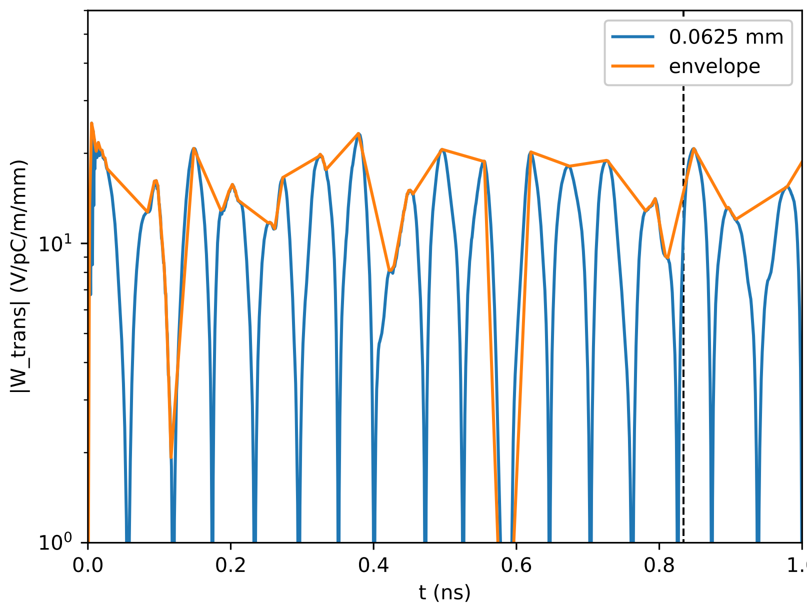

Figure 14: Transverse wakepotential of CompactLight C-band structure.

Constant Impedance Simulations

To better understand how each of the different cell geometries contribute to the final transverse wakepotential, the transverse wakepotential of constant impedance structure models of the first, middle and last cells of the tapered structure were computed. Models with 10 cells were created in Coreform Cubit, exported as .stp files, converted to .stl files using GdfidL's step2stl script and uploaded to Compute Canada's cluster and simulated. The resulting wakes are shown in Figure 16.

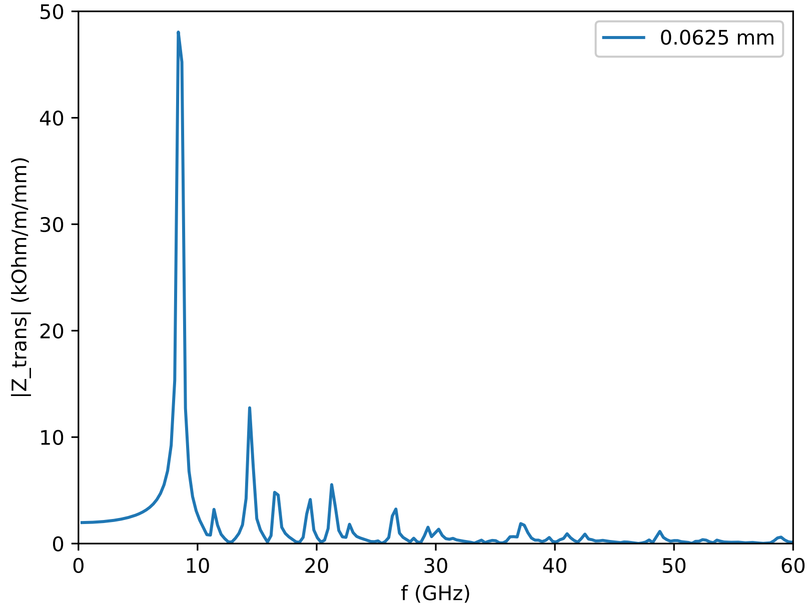

Figure 15: Transverse impedance of CompactLight C-band structure.

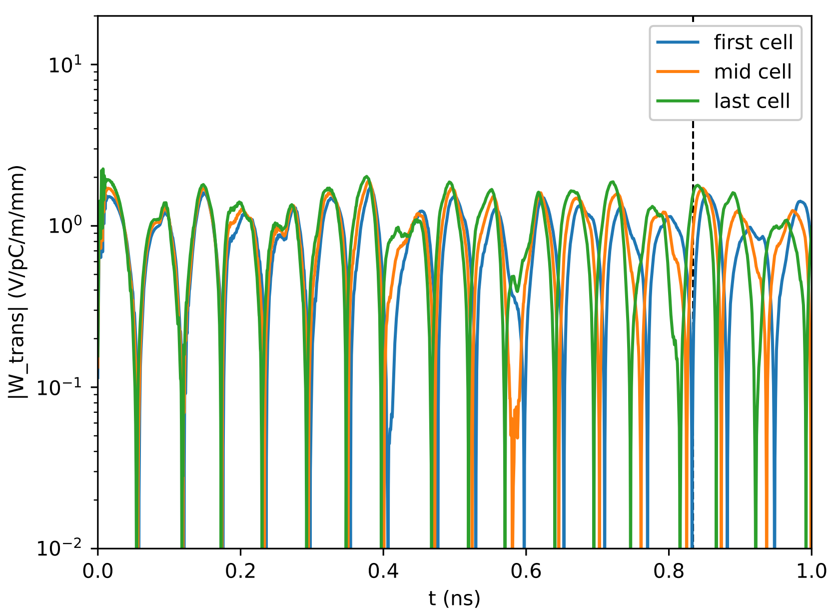

Figure 16: Transverse wakepotential of constant impedance versions of the CompactLight C-band structure.

Shortly following the excitation charge, the wake structures have the same oscillation frequency. For times greater than ~ 0.4 ns, the wake frequencies differ and their minima start to spread. Near 0.6 ns, the spread results in a net minimum of the tapered structure. One can imagine cell geometries between the first and middle cell giving wakes that have minima between the first and middle cell wake minima. The same picture described the wakes of cell geometries between and middle and last cells. Adding the three wakes of the 10-cell structures together and scaling by a factor of four gives the wakes of structure of 120 cells with three constant impedance sections each 40 cells long. The resulting wake is plotted in Figure 17 with the transverse wake of the tapered structure.

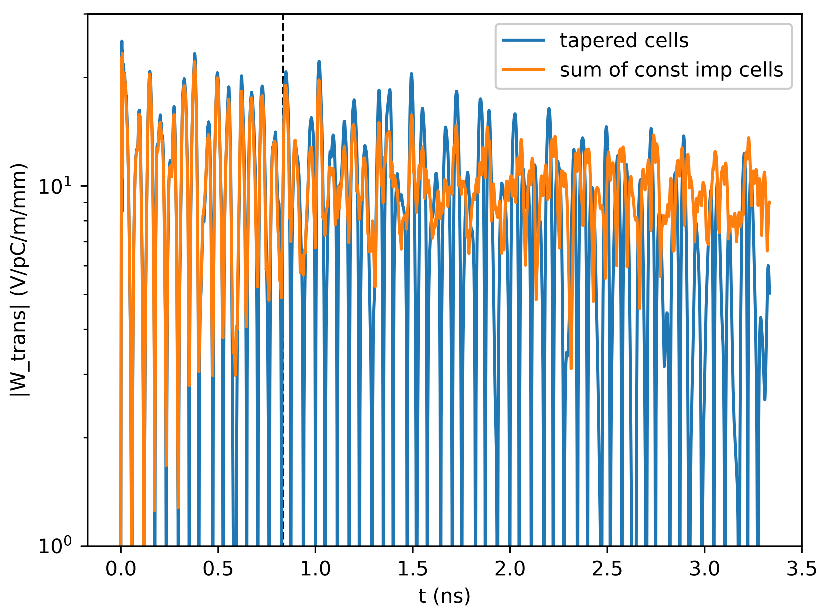

Figure 17: Transverse wakepotential of CompactLight C-band structure and an approximation using constant impedance structure wakes.

The wake generated from the constant impedance structures agrees with the wakes of the tapered structure for a short time following the excitation charge after which the absence of the other cell geometries' contributions to the wakes becomes more noticeable. The different frequency responses of the first, middle and last cells is demonstrated in Figure 18.

The transverse wakepotential envelopes of the X-band and C-band structures are shown in Figure 19. The X-band transverse wakepotential decreases over 1 ns while the C-band wakepotential stays relatively constant. The X-band wake starts at ∼150 V/pC/m/mm

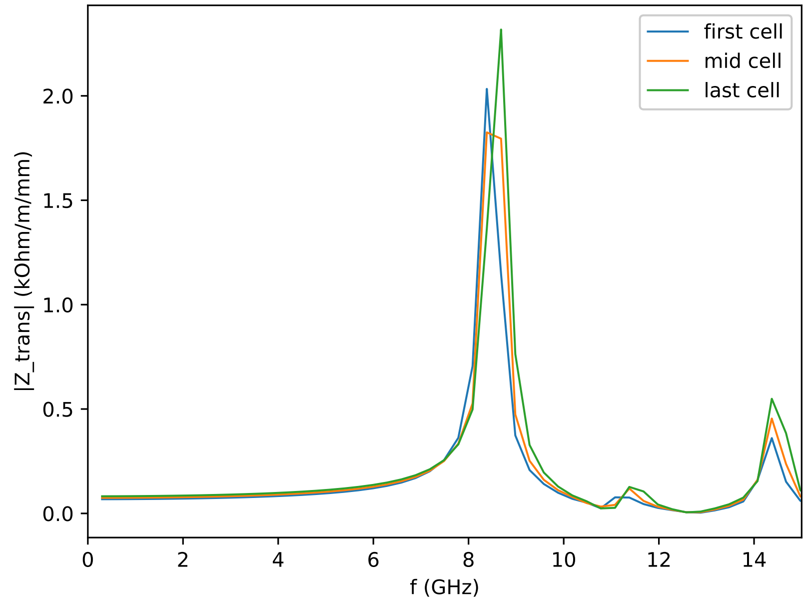

Figure 18: Transverse impedance of CompactLight C-band constant impedance structures.

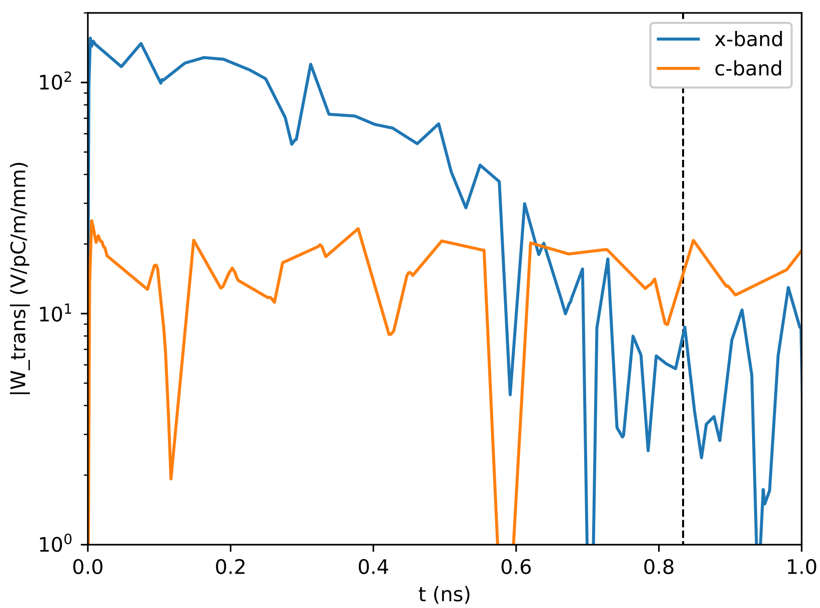

Figure 19: Transverse wakepotential envelopes of CompactLight X-band and C-band structures.

Longitudinal Wakefields

The results of mesh convergence study done on a portion of the accelerating structure shown in Figure 20 indicated a mesh of 0.0625 mm is sufficiently fine to provide accurate longitudinal wakepotentials for the CompactLight C-band accelerating structure.

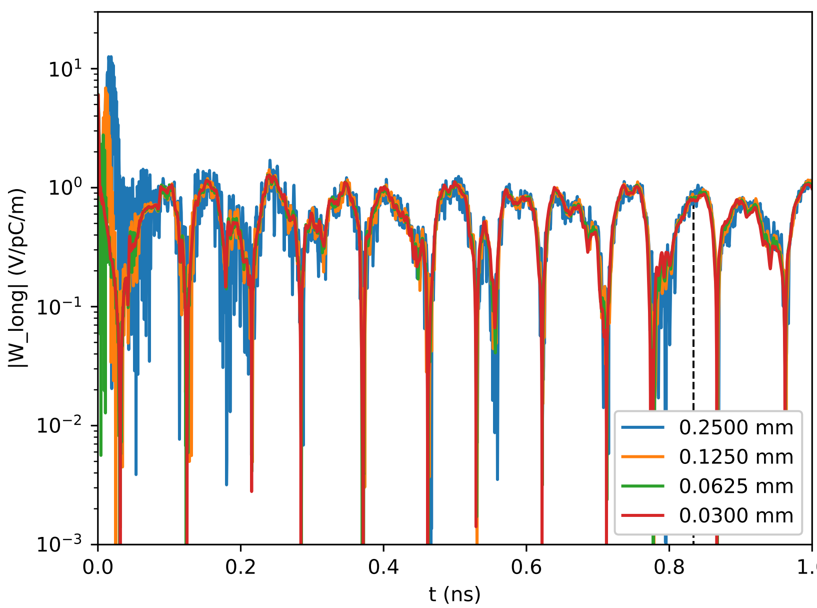

Figure 20: Mesh convergence of longitudinal wakepotential of CompactLight C-band structure using 46 mm of the structure.

Figure 21 shows the longitudinal wakepotential of a C-band structure produced by a bunch with $\sigma = 0.2$ mm and the wake envelope. The wakepotential output from GdfidL had units of V/C. The wakepotential was scaled to V/pC/m by diving the output by the length of the structure and a factor of 4. Since the excitation charge was on two magnetic planes, the simulation was done with a quarter the charge specified in the input and the resulting wakes needed to be divided by 4.

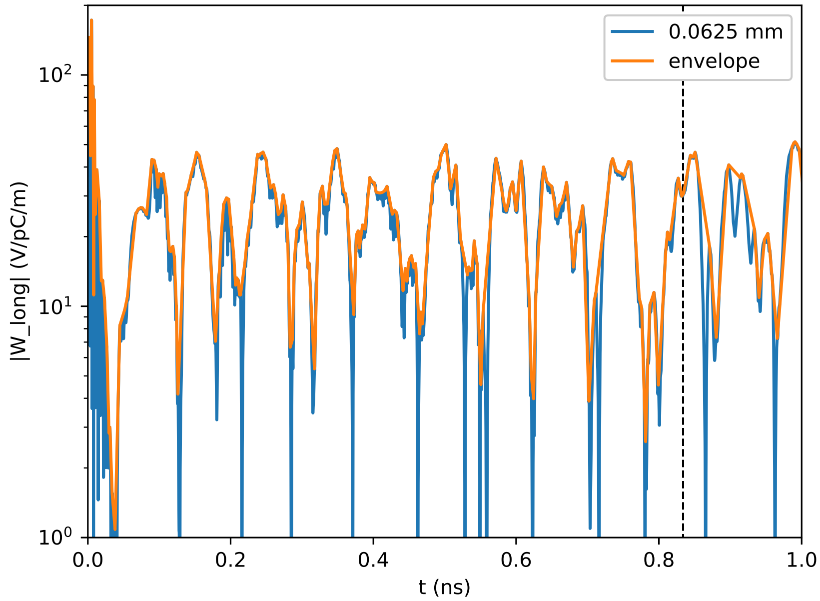

Figure 21: Longitudinal wakepotential of CompactLight C-band structure.

The longitudinal impedance is plotted in Figure 22.

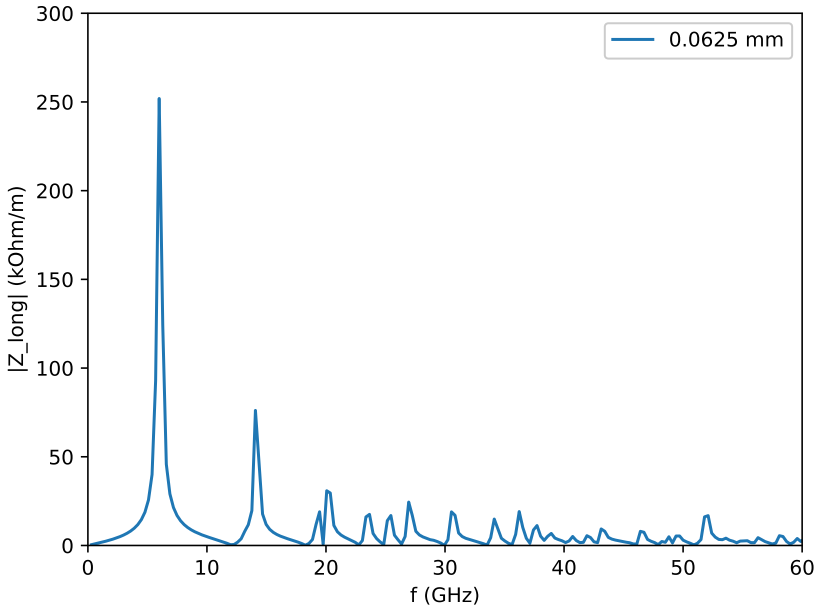

Figure 22: Longitudinal impedance of CompactLight C-band structure.

Future Work

The CompactLight C-band LINAC transverse wakepotential can included in beam dynamics simulations. If the effects from the wakepotential are found to be unacceptable, attempt to minimize the transverse wakes can begin. The current design features a linear distribution of iris apertures along the length of the structure. Models with different iris distributions may be simulated to determine a design with an acceptable transverse wake at the position of the second bunch.

References

[1] G. D'Auria, S. Di Mitri, R. Rochow, A. Latina, X. Liu, C. Rossi, D. Schulte, S. Stapnes, X. Wu, W. Wuensch, H. Castaneda Cortes, J. Clarke, D. Dunning, N. Thompson, W. Fang, E. Gazis, N. Gazis, E. Tanke, E. Trachanas, V. Goryashko, M. Jacewicz, R. Ruber, G. Taylor, R. Dowd, D. Zhu, A. Aksoy, Z. Negris, R. Apsimon, G. Burt, A. Castilla, H. Priem, X. Janssen, J. Luiten, P. Mutsaers, X. Stragier, D. Alesini, M. Bellaveglia, B. Buonomo, F. Cardelli, M. Croia, M. Diomede, M. Ferrario, A. Gallo, A. Giribono, L. Piersanti, B. Spataro, C. Vaccarezza, R. Geometrante, M. Kokole, S. Kyma, J. Arnesano, F. Bosco, L. Ficcadenti, A. Mostacci, L. Palumbo, G. Dattoli, F. Nguyen, A. Petralia, J. Marcos, E. Marin, R. Munoz Horta, F. Perez, Y. Han, A. Bernhard, J. Gethmann, M. Calvi, T. Schmidt, K. Zhang, D. Esperante, J. Fuster, B. Gimeno, R. Hoekstra, A. W. Cross, L. Nix, and L. Zhang, "CompactLight Design Study," in *Proceeding of 10th International Particle Accelerator Conference (IPAC '19)*, pp. 1756–1759.

[2] M. Ferrario, A. Giribono, C. Vaccarezza, J. Scifo, M. Croia, D. Alesini, A. Gallo, M. Diomede, S. D. Mitri, M. Danailov, G. Perosa, Y. Han, A. Latina, W. Wuensch, G. Burt, X. Liu, E. M. Lacoma, A. Mostacci, A. Cianchi, E. Gazis, E. Tanke, N. Gazis, B. Spataro, A. Vannozzi, L. Pellegrino, L. Ficcadenti, G. Pedrocchi, A. Gizzi, M. Behtouei, T. Lucas, B. Gimeno, D. Esperante, and A. Aksoy, "XLS Deliverable 3.4," Tech. Rep. December, 2020.

[3] M. Diomede, *High gradient structures and rf systems for high brightness electron linacs.* PhD thesis, University of Rome La Sapienza, 2019.

[4] W. Wuensch, M. Aichler, D. Alesini, M. Bellaveglia, M. van den Berg, M. Breukers, F. Cardelli, M. Diomede, L. Faillace, A. Gallo, M. Jacewicz, X. Janssen, L. Piersanti, G. Di Raddo, and X. Wu, "XLS Deliverable 4.3," Tech. Rep. March, 2021.